AUTOMATIC WATERLINE REGISTRATION OF A SHIP MODEL IN WAVES

Manases Tello Ruiz, Ghent University-Maritime Technology Division, BELGIUM
Stefan Geerts, Ghent University-Maritime Technology Division, BELGIUM
Guillaume Delefortrie, Flanders Hydraulic Research, BELGIUM
Marc Vantorre, Ghent University-Maritime Technology Division, BELGIUM

Investigation of problems concerning the instantaneous waterline of sea-going vessels requires consideration of several effects, such as squat, bow wave dynamics, wave diffraction and radiation, as well as wave induced motions. Due to the complexity of such problems, (captive) model tests can be considered as a suitable research method, provided that the instantaneous waterline can be determined. Thus, the accuracy of the estimation of the issues involved depends on the proper registration of the waterline. This is usually carried out with image processing techniques, which, if performed manually, mostly result in a tedious work if large series of model tests are involved.

A typical example of such issues is the seakeeping behaviour of so-called estuary (or fluvio-maritime) vessels, i.e. inland vessels that can be utilised for short sea voyages on well-defined trajectories in favourable wave conditions. Besides the strength requirements, the seakeeping results must comply with prescribed values to avoid slamming, green water or flooding of the holds. To investigate these problems, a systematic series of captive model tests was carried out with a 1/25 scale model of an estuary container carrier in the towing tank for manoeuvring in shallow water (co-operation Flanders Hydraulics Research – Ghent University). The tests were carried out in regular waves with different combinations of wave amplitudes and periods, ship speeds and heading angles. During the tests, images of the instantaneous waterline were recorded by an experimental test setup consisting of four black light tubes, a fluorescent coating on the ship model and a computer controlled digital camera.

The large amount of images has to be processed automatically, incorporating new challenges and additional issues such as the varying ship position in waves, causing variations in pixel colour and brightness. The present paper intends to describe a method for identifying the waterline profile based on image processing analysis integrating methods such as correlation analysis and image registration technique.

1. Introduction

Ships are subjected to different loads due to the harsh environment where they operate. These loads can drive hazard on board as well as seasickness, shifting of cargo, slamming, green water. In some scenarios this may lead to the loss of lives and/or the loss of the ship [1]. During the past decades, studies were conducted to assess risk analysis in order to guarantee safety onboard. Examples are the theoretical work of Salvesen et al. [2], largely employed for seakeeping analysis, and the recent application of computational fluid dynamics (CFD) to assess ship dynamics [3].

Although those methods often lead to a good approximation, their accuracy concerning the instantaneous position of the actual waterline in operational conditions is not always sufficient. Therefore, values for seakeeping criteria prescribed by maritime authorities to ensure crew and ship safety are often conservative.

To enhance the theoretical methods, the complex environmental conditions suggest the incorporation of several non-linearities so as to attain suitable results for the physical problem. For example, such non-linearities can be related to the order of magnitude of the wave amplitudes

(considered small for linear theories) or to the mean shape of the hull below the waterline [4]. The incorporation of such effects leads to highly elaborate methods, which require higher hardware capacity and increased computational times for an often slight enhancement. Therefore, new methods should be investigated.

Two relevant problems of seakeeping, shipping of water on deck or in open holds and slamming criteria, are often only approximately predicted by numerical methods. These phenomena are associated to the local freeboard and the local draught to be determined with respect to the waterline. Thus, the accurate determination of the waterline location is of critical importance. For this purpose, methodologies based on images seem suitable since images permit to identify, by visual observation, features and states of moving objects recorded on an specific moment .

Image analysis is not a new concept, it has already been employed in different fields, e.g. in medical analysis [5] and in geographical information systems known as GIS. In fact, image processing is neither uncommon for the analysis of problems related to ship hydrodynamics [6], [7]. Such techniques have already been employed to measure the influence of the wave elevation along the hull of a sailing yacht in the frame of resistance prediction [8]. However, as reported by [9], up to now, studies involving this methodology are often carried out manually, image by image, resulting in a tedious work if a large set of images is considered.

If the images are recorded with a sufficiently short time interval so as to capture the shape of the waterline quasi continuously, large sets of images are the result of one single test run. Thus, considering an entire test program, a manual analysis is not an option. Automatic image processing is necessary; this however will bring in new challenges such as the variation of pixel intensities within each image, and defining ship edges and the waterline at different locations within the image frame.

To investigate this method, captive model tests have been conducted with a 1/25 scale model of an estuary container carrier in the towing tank for manoeuvring in shallow water (co-operation Flanders Hydraulics Research – Ghent University) in Antwerp, Belgium. Different combinations of wave amplitudes and periods, ship speeds and heading angles were tested. During each test, images of the instantaneous waterline were recorded by an experimental test setup consisting of four black light tubes, a fluorescent coating on the ship model and a computer controlled digital camera. An extensive discussion of the experimental set up can be found in [9].

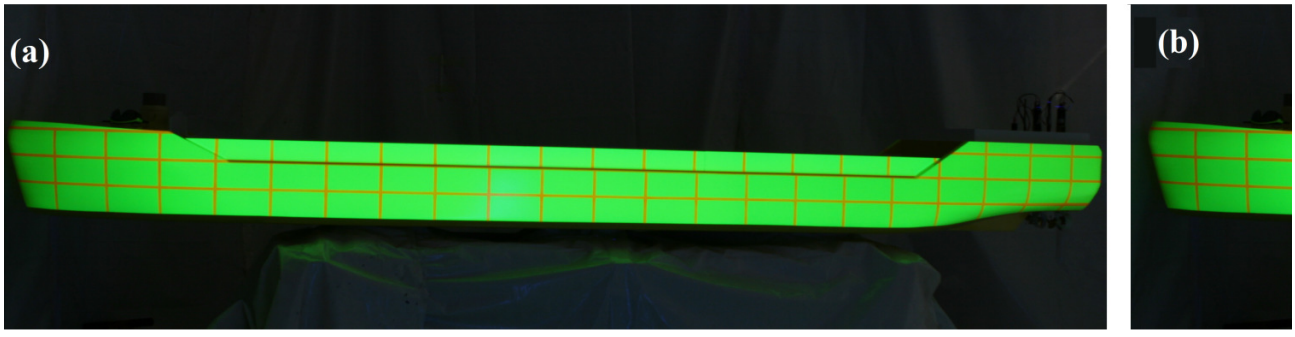

Fig. 1 Model of the estuary vessel (left) and bow section chosen for analysis (right)

The hull model is painted with a projected Cartesian mesh to permit the further registration of the waterline. A profile view of the ship hull is shown in Fig. 1a.

In the present study, four cameras were used to record the instantaneous waterline over the whole ship length, one camera at the bow, another at the stern and two to cover the sections in between.

However, since the purpose of the present work is to investigate a methodology based on image processing, the area of interest will be restricted to images from the bow section, Fig. 1b. An example of this image can be seen in Fig. 2.

To attain the automatic identification of the waterline profile problem, the present work is based on image processing analysis, incorporating methods such as correlation analysis and image registration technique, thresholding and morphological operations. Additionally, for a better understanding, the analysis for the detection of the waterlines is conducted in four steps:

- image borders detection
- control-point pairs
- image registration: spatial transformation, and
- freeboard estimation

Techniques such as registration and correlation are needed to map the input image to a non-distorted reference image or orthogonal photo, hereafter called *ortho-photo* where measurements can be taken and further analysis related to local freeboard and draught can be conducted. A discussion of the methods and algorithms employed in the present work is given in the following section.

2. Outline of waterline registration by image analysis

The test setup consisted of four black light tubes, a fluorescent coating painted on the ship model and a computer controlled digital camera (more details of the experimental test can be found in [9]). The setup has been designed in order to simplify the image analysis method by reducing glare and noise, and increase the light intensity from the ship model to the camera. The main particulars of the estuary vessel model are given in Table 1.

Table 1 Ship main characteristics, model scale

Length over all	[m]	4.40	Draught	[m]	0.15
Length between perpendicular	[m]	4.25	Depth	[m]	0.23
Breadth	[m]	0.68	Scale	[-]	1:25

2.1. Colour spaces

As the colours chosen for the ship model coating are approximately red and green, a consequent decision is to employ the RGB colour space. This is supported by the large intensities found in the red and green sub spaces, Fig. 2. This increases the contrast of the ship's features in respect to the water and the background. As the blue sub space does not present any relevant information, it is omitted and further work will only take into account the red and green sub-spaces.

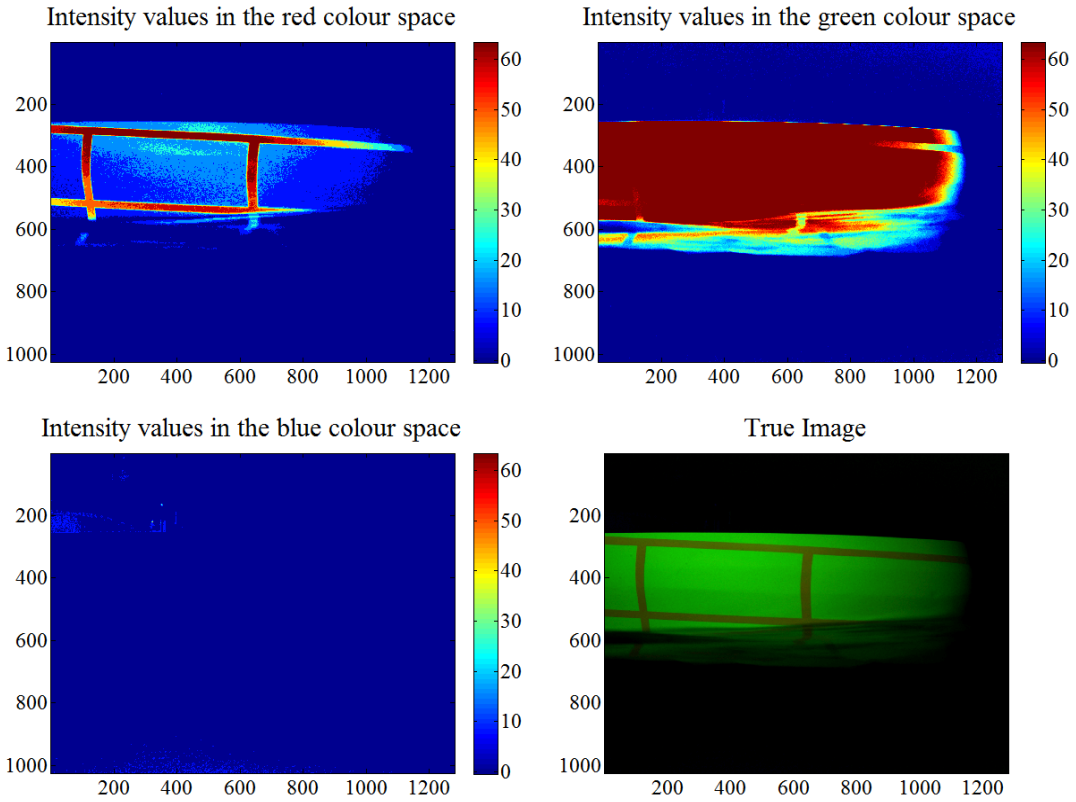

Fig. 2 Colour intensities shown in the legends (left side of images) for the red, green and blue colour spaces. Image dimensions of 1280x1024 pixels.

2.2. Methodology

As mentioned above, the present approach separates the problem into four sub-analyses. First, the analysis starts with *image borders detection* and *control-point pairs*. Then the outputs are input to the *image registration* and finally to the *freeboard estimation*. These steps are shown in Fig. 3.

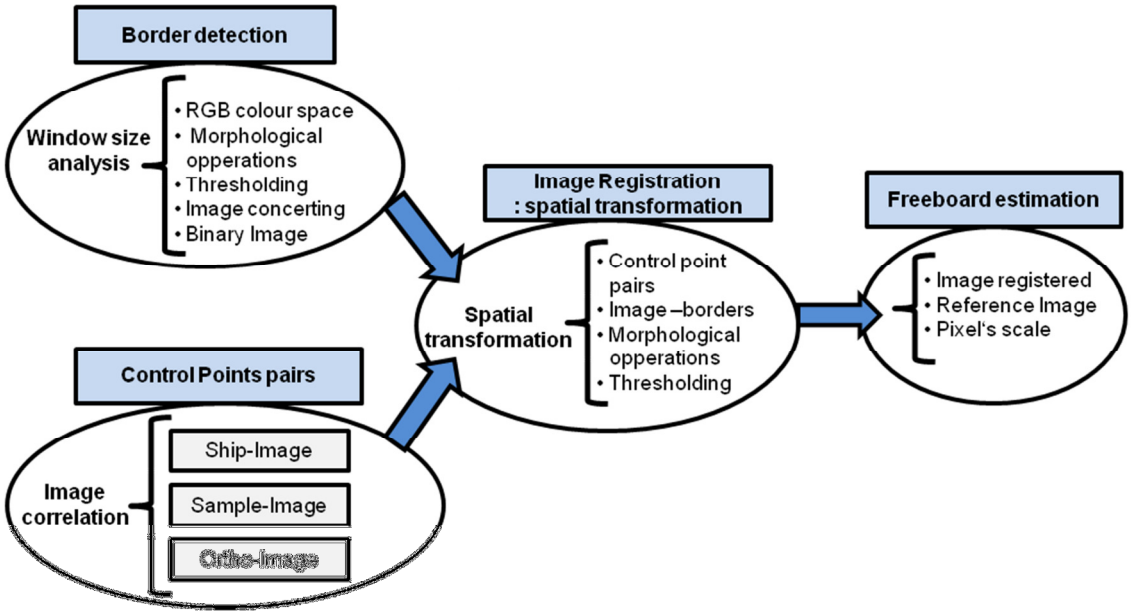

Fig. 3- Illustration of the image analysis

The border detection delimits the ship from the background thus identifying the waterline profile. The control-point pair determinates locations of specific features in the ship to be used later in the spatial transformations. The latter maps the input image to the space of the reference image, i.e. measurements can be taken.

The automatic waterline detection and the control-point pair location are the most difficult problems to solve in the present work. Since it is required to handle a large set of images, this involves an inherent problem related to the pixels variation defining the location of the ship at different regions within each image frame, thus, the waterline and the control points differ for all images.

Additionally, a smooth variation of pixel intensities at the bow of the ship and higher pixels intensity at the water surface (reflection problem, see Fig. 2 for green space) are found. These problems will consequently reduce the contrast between the image and the background making the identification of the waterline more difficult. Hence, any direct application of edge detection methods, such as the Canny method, or the Sobel and Prewitt methods [10], seems impractical. This implies that the automatic identification of the ship borders and the control-point pairs requires a special treatment.

2.3. Image borders detection

Processing the entire image brings in several difficulties such as the reflection and the continuous variation of pixel intensities, Fig. 2. Subsequently, edge detection methods cannot be applied directly thus a more suitable approach should be employed. An alternative method incorporating basic tools of image analysis is developed. This methodology consists of:

- first, the initial position of the window is given.
- second, the image is cropped to the size delimited by the given window element.
- third, by thresholding, the cropped image is converted from a true colour image to a binary image.
- fourth, the borders in the binary image are identified and recorded.
- finally, the new position of the window is updated. This analysis is conducted until the whole image has been processed.

For a better understanding, an illustration of the method is presented in Fig. 4.

The present methodology involves an automatic variation in the position of the window element. Considering the sketch presented in Fig. 5 for the iterations $n-1$, n and $n+1$. To carry on the present work, two coordinates system are employed, which are: the picture bound coordinate system OXY and the window fixed coordinate system pxy. OXY is fixed for all the images while the pxy systems move along the image as borders are detected. Both axes systems are parallel to each other.

The automatic variation of the window element is achieved as follows:

- first, the moving window detects the borders shown in black in the step n, then
- the extremes are found and labelled as “1” and “2”, and
- finally, the centroid of the window is move to the new position $“2”$ for the next interaction $n+1$.

Detecting points $“1”$ and $“2”$ is a simple task to achieve since they belong to the edge of the cropped image. Their labelling as “1” or “2” is based on their distance to the points of the border previously

detected. This distinction is based on the criterion of maximum distance. For the very first step of the entire analysis the detection of the points is a special case. In this scenario, the criterion is based on the distance from the origin in the x- global coordinate system,$OXYZ$ (see Fig. 5).

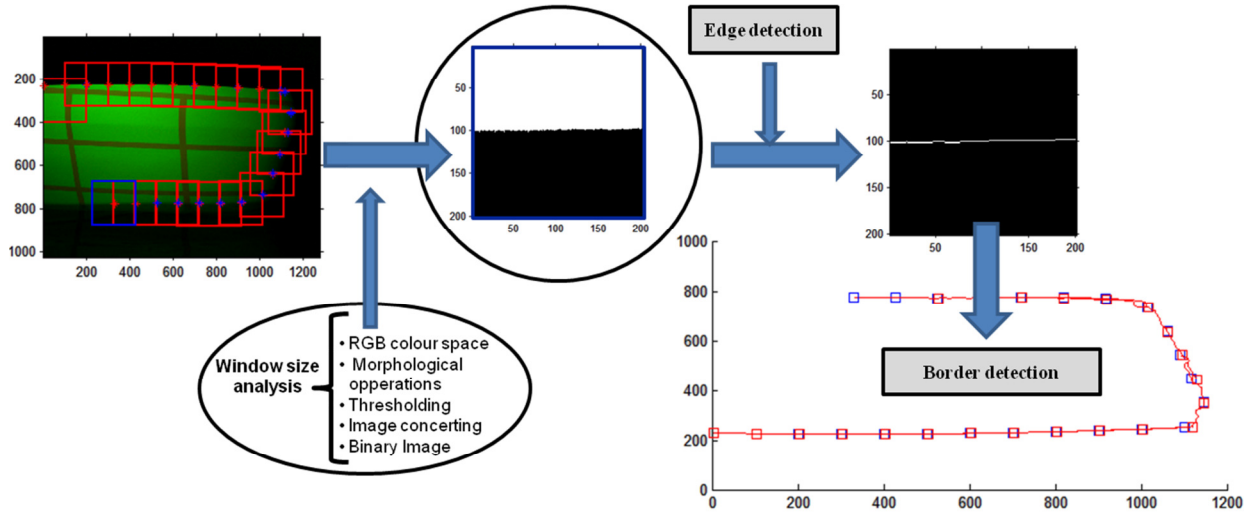

Fig. 4 Illustration of the proposed border detection

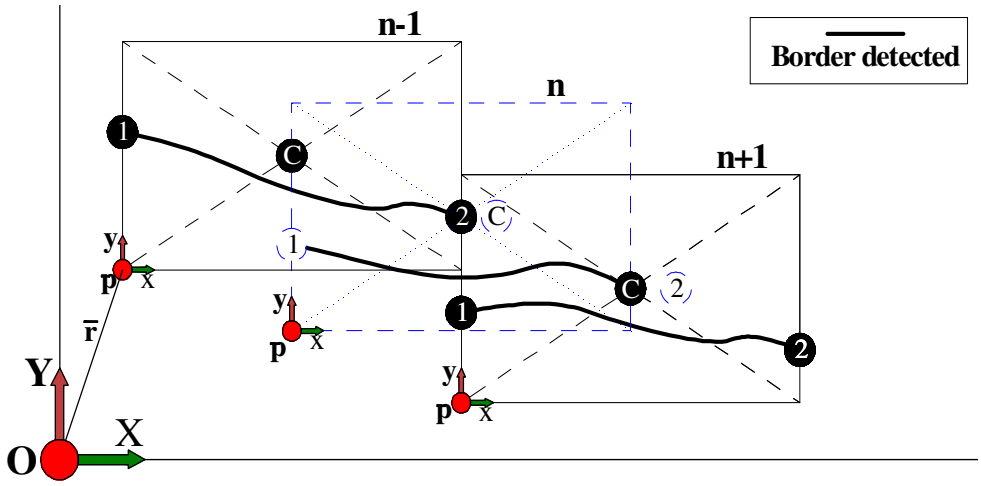

Fig. 5 Iterative processes of border detection

The window element with the size of 80×50 pixls has been employed in the present analysis. This size has been chosen to avoid noise from the background such a reflection, and also to provide sufficient distinction between the ship hull and the background.

An example of the results of the application of the present method for a sample image can be seen in Fig. 6. The images size is 1280x1024 pixels, the border detected binary image and the true colour image with the borders superposed (in red colour) are presented at the left and the right of Fig. 6 respectively.

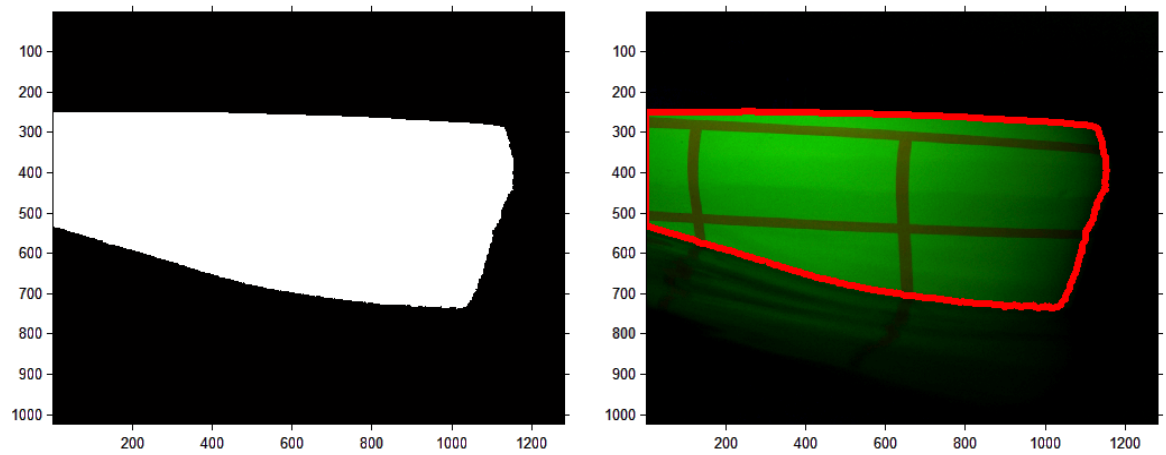

Fig. 6 Results of the image processing for border detection. Image size of: 1024x1280 pixels.

2.4. Control-point pairs

The control-point pairs can be any particular feature, within the image and the ortho-photo, unique for both images. To identify these particulars a mathematical approach based on image registration and a match or similarity measure based on the normalized cross-correlation (NCC) are employed. In the present work, the NCC formulation presented in [11] and implemented in Matlab under the function name *normxcorr2* is used. The function requires two images: a template-image and the image for correlation (herein only refer to as image). In the NCC method the template-image is shifted at different location within the image, subsequently at each location the normalized cross-correlated values are calculated by (1):

$$\gamma(\mu,\upsilon) = \frac{\sum_{x,y}\left[f(x,y) - \bar{f}_{\mu,\upsilon}\right]\left[t(x-\mu,y-\upsilon) - \bar{t}\right]}{\left\{\sum_{x,y}\left[f(x,y) - \bar{f}_{\mu,\upsilon}\right]^2 \sum_{x,y}\left[t(x-\mu,y-\upsilon) - \bar{t}\right]^2\right\}^{0.5}} \tag{1}$$

Where $\bar{t}$ is the mean of the template and $\bar{f}_{\mu,\upsilon}$ is the mean of $f(x,y)$ of the region of the image under the template. The variables μ,υ are the displacement, in rows and columns respectively, of the template over the image. The values of $\gamma(\mu,\upsilon)$ vary between -1 and $+1$.

To conduct the present work two templates where needed: a T-shape and an Up-corner shape. The decision to employ two templates is based on that both describe unique and distinguishable features in the images. The T-shape is a particular feature with only two occurrences localized in the upper part of the image. Whereas, the Up-corner shape represent a general and unique characteristic for the lower horizontal lines with at least four occurrences.

One can argue that for the lower lines, the cross intersections or the down-corners shape can be used indistinguishable. However, this does not hold true. Employing the cross intersection or the down-corner, a lower NCC values will be found when the waterline passes through the intersection of the lines, whereas, this scenario will still gives higher NCC values if the Up-corner shape is used. The template images, the NCC values, and the superposed image with the templates are plotted in Fig. 7.

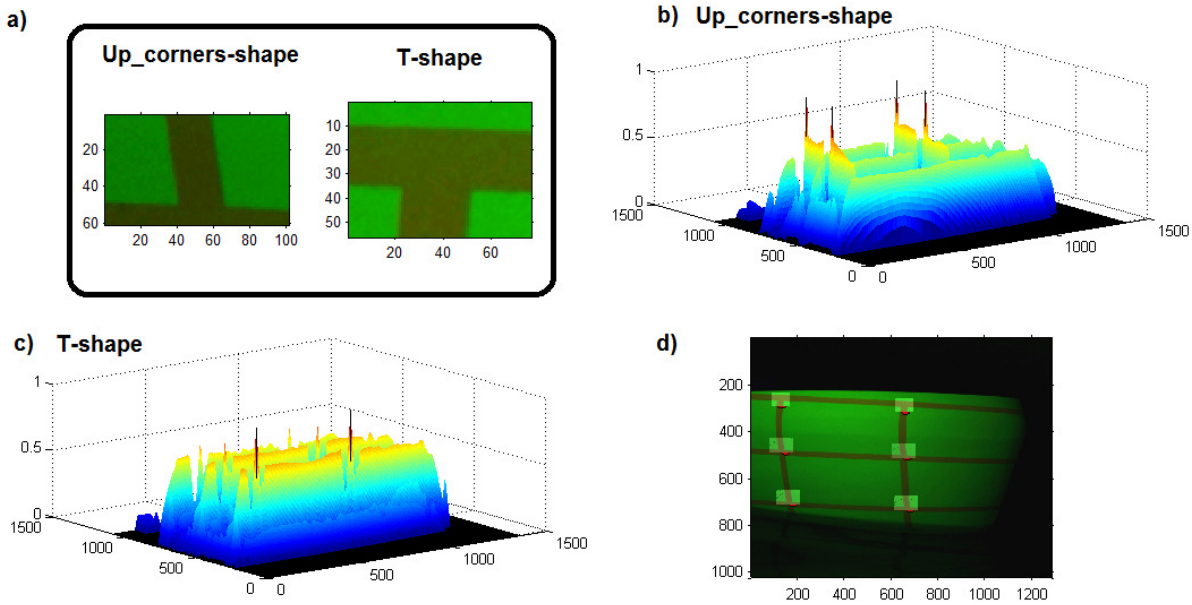

Fig. 7 (a) Image templates, the Up-corner and T-shapes, (b) NCC for the up-corner shape, (c) NCC for the T-shape; and (d) superposition on templates on the image

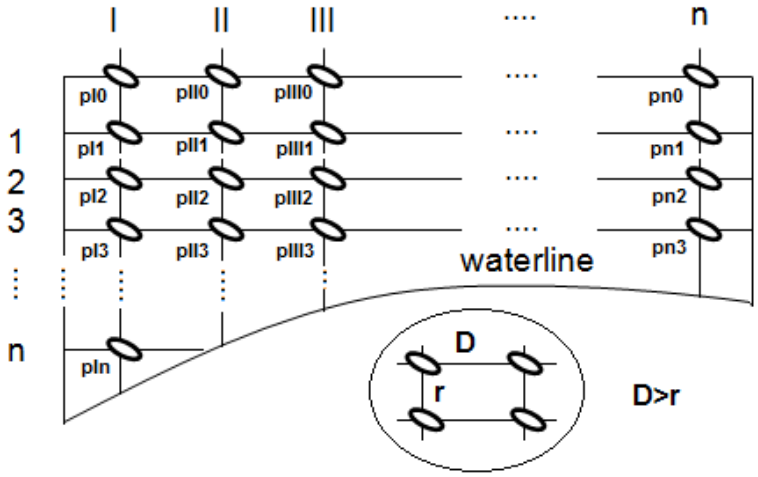

Fig. 8 Points order for matching

Once the matching points have been found, the following step is to relate them to the same particular in the ortho-photo image (see Fig. 9). To match the image points and the ortho-photo points, an algorithm based on the layout of the lines has been developed. First, the corresponding points, in the range of the image, belonging to the ortho-photo are selected and labelled as illustrated in Fig. 8. The second step is to organize the points detected in the image. This is achieved by:

- first organizing the located T-shape points (first row in Fig. 8) as a function of the distance to the image's origin, then
- the $px1$ ($x = I, II, III \ldots n$; y = 1,2,3…) points are ordered as a function of the distance to the T-shape points with the constraints of distances D and r, then
- the $px2$ ($x = I, II, II \ldots n$) points are ordered as a function of the distance to the $px2$ with the constraints of distances D and r. This process is run until all the points identified are matched.

An illustration of the matched points, plotted in the ortho-photo and the image, is presented in Fig. 9. The correspondence between the points is given by the colours and shapes. Note that two points are

plotted for each found location. Those points, marking the image-corners of the templates, are required due to the lack of control points to apply the polynomial transformation (see section 2.5).

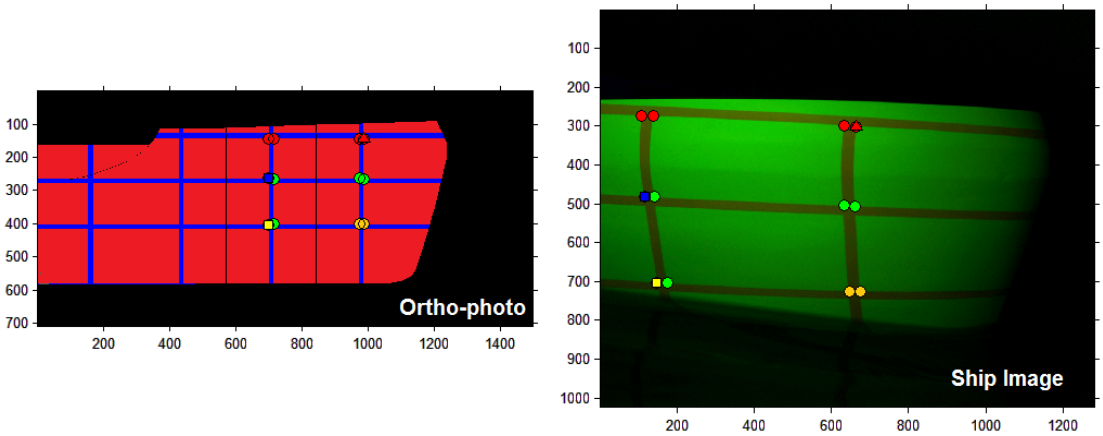

Fig. 9 superposition of the control point pairs in: the ortho-photo (left) and the Image (right)

2.5. Image registration: spatial transformation

In the present work image registration is employed to fuse the images obtained in the tests and the ortho-photo. An illustration of this method is presented in Fig. 10. Consider the image “A”, with vertical lines, and the image “B”, with horizontal lines, both of the same object; however with different features. Additionally, image “A” presents a relative distortion in respect to “B” (the distortion can be addressed to the view angle of the object). Thus, mapping image “A” to the space “B” and fusing them results in an image which includes the relevant information of "A" and "B".

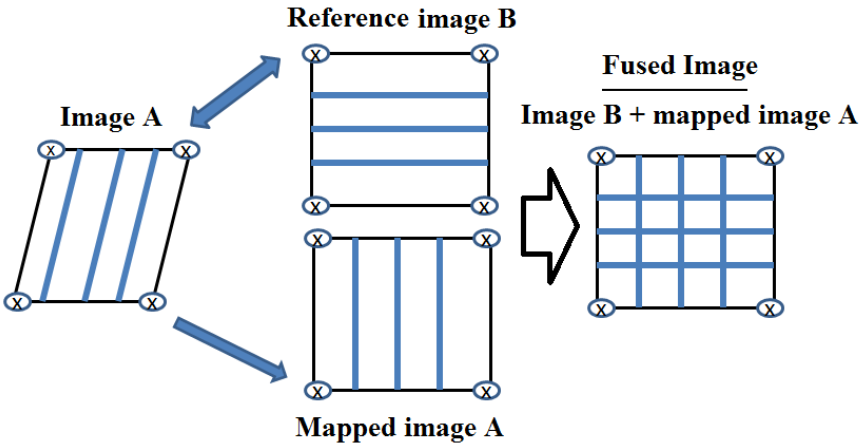

Fig. 10 Image registration and fusion between the mapped image and the reference image

As the present task is to determine the local freeboard and draught, this measurement can be retrieved if the test images are fused in to a profile view of the ship hull (ortho-photo). However the proposed spatial transformation is of a two-dimensional type. This, as mentioned by [12] will introduce errors as different planes of the three-dimension space, described in 2D a image, will require different spatial transformations. Thus, 2D spatial transformation applied to the ship images seems unsuitable.

Nevertheless, as the objective is to register the waterline into the profile view of the ship, mapping the entire image is not relevant. The fraction of the image of concern is the area where the waterline is defined. Besides, as the ship is partly submerged, the most flat part of the hull remains above the

water surface. This will decrease the three-dimensional effect on the images and reduce the error while applying this methodology. Moreover, if the control points near the waterline are chosen for the registration, a 2D transformation would not induce significant errors.

To perform the registration, the present work uses the Matlab functions *cp2tform* and *imtransform* implemented both in the image processing tool, and the profile view of the ship as the ortho-photo. The type of spatial transformation depends of the relative distortion of the input image relative to the output image. In the literature, several types of 2D spatial transformation are available, such as affine, projective and polynomial transformations.

In the present work 2D projective and polynomials transformations are employed, because of the relative distortion of the images (see Fig. 11) with respect to the output image (see Fig. 9, ortho-photo). Thus, Fig. 11a,b seems suitable for the polynomial transformation while Fig. 11c for the projective transformation.

The 2D projective transformation is a linear transformation and does not preserve parallelism between lines, neither angles nor proportions [12]. This method, also known as homography, employs homogenous coordinates systems. The homogeneous coordinate system, (x'', y'', z''), is a modification of the Cartesian coordinates, (x', y'), where the third cordinate z'' has been introduced for mathematical simplification. By the employ of the homogeneous coordinates, the spatial transformation of the 2D image form input plane to the output plane is given by:

$$(x', y') = (\frac{x''}{z''}, \frac{y''}{z''}, 1) \rightarrow (x'', y'', z'')$$

$$\begin{bmatrix} x'' \\ y'' \\ z'' \end{bmatrix} = \begin{bmatrix} H_{11} & H_{12} & H_{13} \\ H_{21} & H_{22} & H_{23} \\ H_{31} & H_{32} & H_{33} = 1 \end{bmatrix} * \begin{bmatrix} x \\ y \\ z \end{bmatrix} \quad (2)$$

The value assigned to the third element of the matrix transformation, $H_{33} = 1$, is due to the relationship between the homogeneous and the Cartesian coordinates. Hence, only eight variables are unknown in the present method consequently only four control points are required for this method.

The polynomial transformation is used when curve distortions between the image and the reference image are observed. The order of the polynomial will depend on the degree of distortion of the images with respect to the reference image. This method should be carefully used since polynomials can rapidly change their tendency thus introducing unexpected results. The present work, a polynomial of second order is employed. The relationship between the input image space,(u, v), to the output image space, (x, y), is given by:

$$u = k_1 + k_2 x + k_3 y + k_4 xy + k_5 x^2 + k_6 y^2$$

$$v = k_7 + k_8 x + k_9 y + k_{10} x * y + k_{11} x^2 + k_{12} y^2 \quad (3)$$

Thus considering the number of variables, to map the input image to the output image at least a minimum of 6 points of control pairs are required.

However, Fig. 11b does not comply with the minimum required control-points pairs for the polynomial transformation. To overcome this difficulty a practical solution was adopted. This is to increase the number of control-point pairs in twice the number of template matches. This is not the best solution but it is a necessary action due to the lack of particular features in the images. Hence, the present work uses the polynomial transformation for images such as Fig. 11a,b and the projective transformation for others like Fig. 11c.

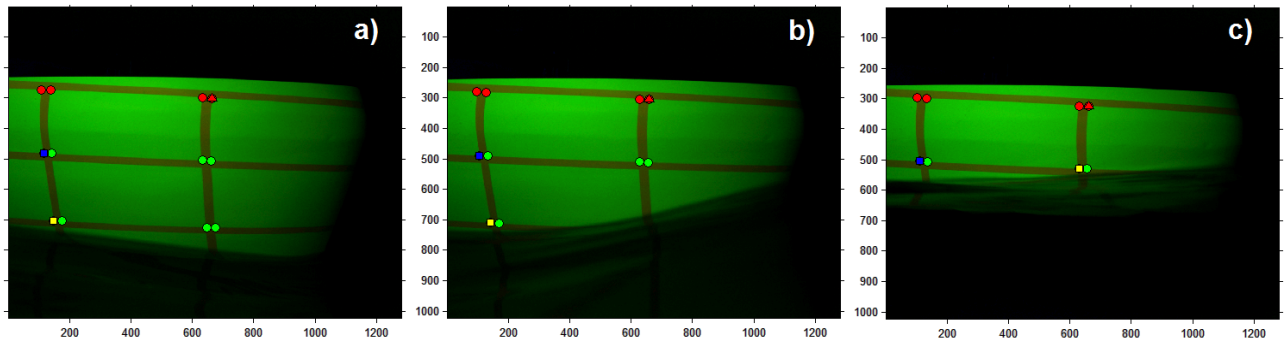

Fig. 11 variation of the number of control-point pairs in the images

Fig. 12 shows the results of the transformed image fused with the reference ortho-photo. To accomplish this, the polynomial transformation of second order was used. Note, the image only represents the bow part of the ship and it is displayed in Fig. 12 by the black curved area.

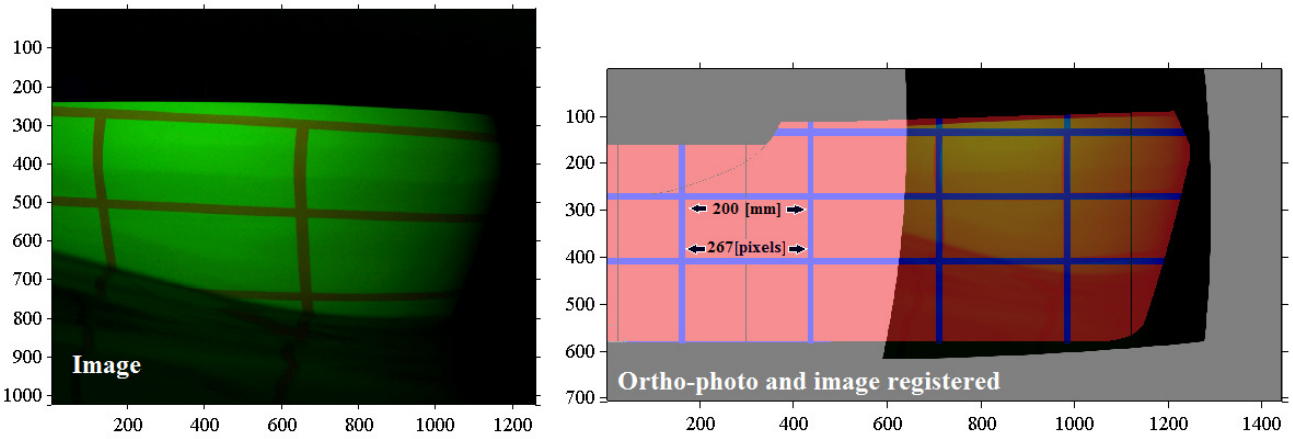

Fig. 12 Illustration of image registration, Image (left) and ortho-photo and superposed image (right)

As observed in Fig. 12 a clear position of the waterline can be identified. It is also observed that now the blue vertical lines of the ortho-photo and the lines of the image are superposed. This indicates a good agreement while employing the polynomial of second order for the spatial transformation.

2.6. Freeboard estimation

To determine the local and instantaneous values for freeboard and draught, the registration and fusion of the true-colour images with the ortho-photo is not sufficient. To accomplish this task, the same procedure is required with their respective binary images. The spatial transformation of the binary images follows the mathematical procedure inferred from the true colour images. In Fig. 13 the binary images of the respectively true colour images presented in Fig. 12 is shown.

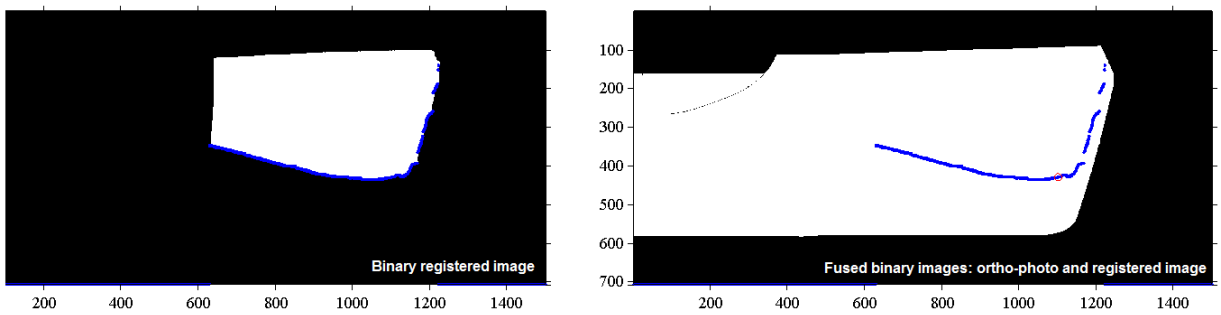

Fig. 13 true colour and binary images registered, image resolution of 1498x709 pixels

Morphological operations are further used to distinguish the waterlines from the ship borders. The application of such methods for several images lead to a better representation of the waterlines. The following step is to convert the dimensions in pixels to meters. To this purpose, a scale is drawn from the known dimensions, in pixels and metres, of the squares in the ortho-photo (see Fig. 13*)*. The scale factor for the conversion from pixels to meters for all images registered and mapped into the space of the ortho-photo is given by:

$$scale = \frac{200}{267} \approx 0.75 * 10^{-3} \left[{}^{meters}/_{pixels} \right] \qquad 4$$

Additional to the scale factor conversion given in Eq. 4 a vertical offset is introduced for a better representation of results. The resulting figures with the registration and superposition of the waterlines for tests WA50 and WM11 are presented in Fig. 14. The wave characteristics are given in Table 2.

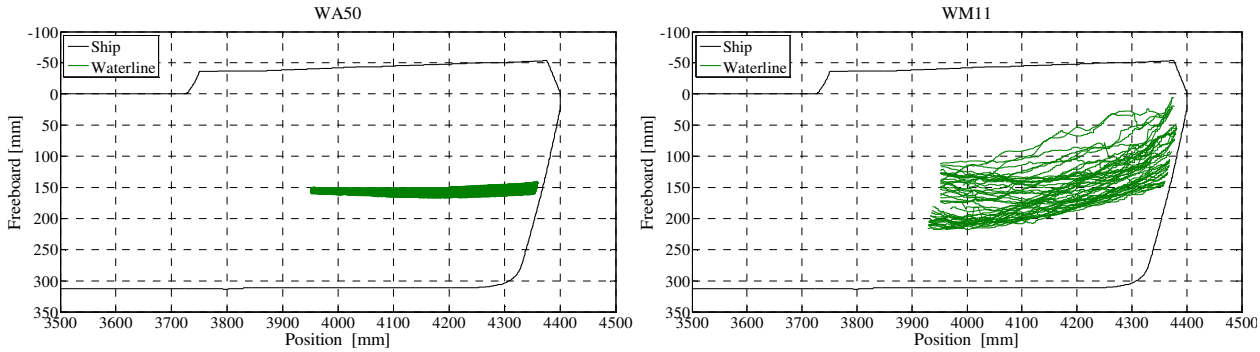

Fig. 14 waterline registration at zero speed (left) and non-zero speed (right), model scale.

In the figure, several waterlines have been detected and superposed one after another. The more disperse location of the waterlines (green lines) for test WM11 indicates a more severe behaviour of the ship than for test WA50. Whereas, the lower disperse waterlines for test WA50 indicates the ship behaves similarly to the behaviour in calm water (see Table 1). Moreover, the result permits to .identify critical values for the local freeboard and the draught. Thus, the presented method is suitable to solve the present problem.

3. Results and discussion

The analysis takes into account wave characteristics typical for the zone where the estuary ship is most probable to navigate [13], Table 2. In Table 2 the heading angle follows the standard

convention of seakeeping analysis, this is: 0°, 90° and 180° for following, beam and head waves, respectively.

Table 2 Regular wave characteristics

Name	Wave amplitude [mm]	Period [s]	Velocity [m/s]	Angle of incidence [°]
E0102G01_WA50	19.5	1.0	0.00	0
E0102G01_WA51	19.5	1.2	0.00	0
E0102G01_WA54	19.5	1.2	0.00	50
E0102G01_WA59	19.5	1.0	0.00	135
E0102G01_WA62	19.5	1.0	0.00	180
E0102G01_WL88	40	1.0	0.36	10
E0102G01_WL90	40	1.2	0.36	10
E0102G01_WM11	26	0.8	1.08	190
E0102G01_WM12	26	0.9	1.08	190
E0102G01_WM13	26	1.0	1.08	190

Fig.15 and Fig. 16 present the results for tests given in Table 2. It is important to mention that the results have been filtered to avoid wrong estimations of the waterline. Examples of those erroneous estimations can be observed in Fig.15 for test WA59 and in Fig. 16 for test WL88 and WL90. They have been analysed independently to identify whether they contain any relevant information.

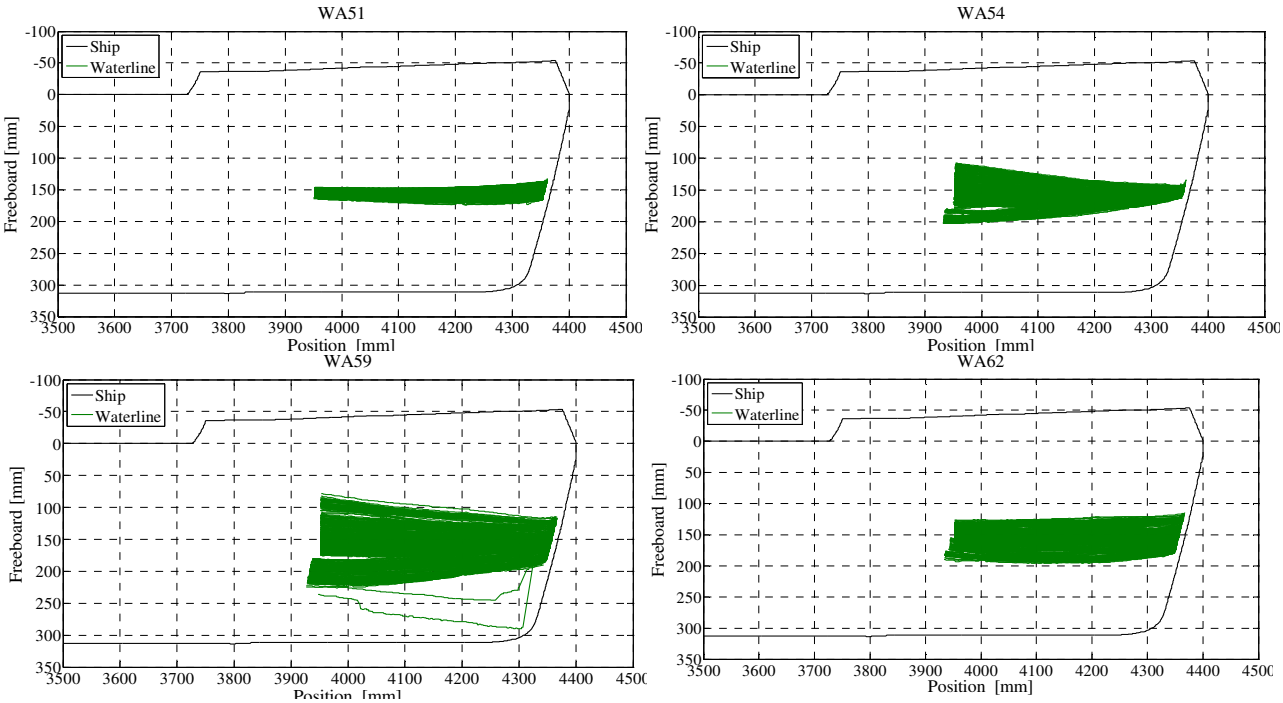

Fig.15 Waterline registration at zero (left) and non-zero (right) ship speed, model scale

In Fig.15 and Fig. 16, the registered waterline describes regions within the ship profile view, as observed for the test cases presented in Fig. 14. The waterline delimits the ship profile view and the determination of the local freeboard and draught is reduced to a simple observation.

From Fig.15, test WA51, a smaller region delimit by the waterlines is observed. These results are similar to the ones obtained for test WA50 (see Fig. 14) even though a different wave period was

chosen, similar results are found for test with non-zero ship speed, see tests WL88 and WL90 in Fig. 16. However, a change in wave direction, see tests WA54 and WA59 Fig.15, or an increased ship speed, see test WM12 and WM13 in Fig. 16, increases the area delimited by the waterlines considerably.

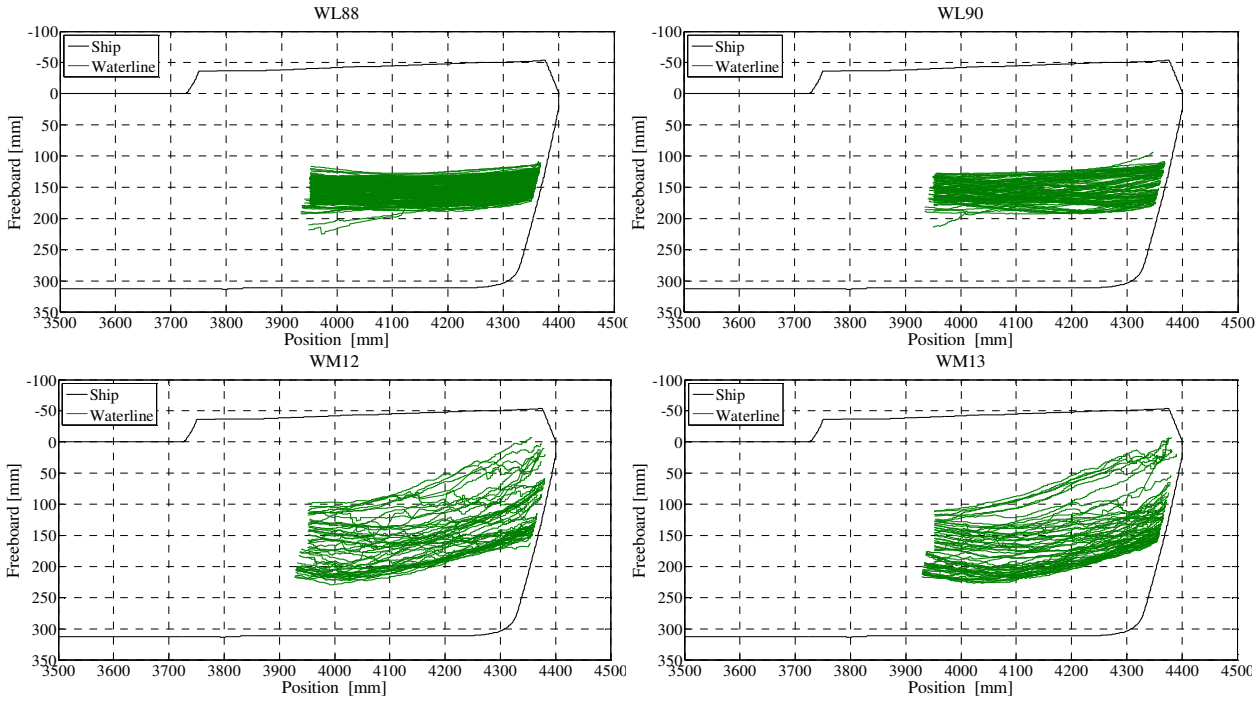

Fig. 16 Waterline registration at non-zero ship speed, model scale

Additionally to the observations made above, In Fig.15 and Fig. 16 two critical locations for the freeboard can be identified: first at the bow of the ship and the second at around 10% Lpp (measured from the bow towards astern, see Fig.15, e.g. WA54 and WA62). The first one occurs for tests with ship speed and increases as the ship speed is increases. Whereas, the second one occurs for test at zero ship speeds. Similarly, lower draughts are found at around 10% Lpp, independent of the ship speed.

The ship speed and quartering waves indeed induce higher probability of hazards and dangerous conditions. Those observations apparently validate the reliability of the present method since the results agree with theoretical seakeeping observations such as the impaired ship operability as a consequence of increasing the ship speed or sailing in quartering waves [14].

Hence, the present method permits to identify precisely the freeboard and the draught over the length of the ship. This will represent an advantage to assess seakeeping performances such as green water on deck and slamming criteria. Therefore, considering what has been stated above, the present method based on image analysis to assess seakeeping performances seems a suitable approach.

4. Conclusion

The present work is an attempt to analyze of the local and instantaneous freeboard and draught based on standard image analysis tools, by employing correlation analysis, image registration and morphological operations. Several difficulties have been faced with while dealing with the

waterline registration such as the border detection and the identification and matching of control-point pairs.

Constraining the border analysis to a small region of interest reduces the noise effects and simplifies the identification of the waterline. Thus, the window-size analysis employed in the present work seems a suitable method for border detection. Additionally, the identification of the control-point pairs based on the normalized cross-correlation permits to easily localize particular features within the image and does not require any additional processing. These two methods are the base of the present work. Therefore it can be stated that the automatic waterline registration based on standard image processing tools can be employed to assess risk analysis associated with freeboard and draught.

5. References

1. L. Pérez Rojas, F. P. Arribas, R. Z. Rodrıíguez, and A. G. Pacheco, (2006), "On the accidents of small fishing vessels," in Proceedings STAB2006.
2. N. Salvesen, E. O. Tuck, and O. M. Faltinsen, (1970) ,"Ship motion and sea loads," Transactions SNAME, vol. 78.
3. P. Ferrant, L. Gentaz, C. Monroy, R. Luquet, G. Ducrozet, B. Alessandrini, E. Jacquin, and A. Drouet, (2008), "Recent advances towards the viscous flow simulation of ships manoeuvering in waves," in Proc. of 23rd Int. WWWFB.
4. N. Fonseca and C. Guedes Soares, "Time-domain analysis and wave loads of large-amplitude vertical ship motions, (1998), "Journal of Ship research, vol. 42, no. 2, pp. 139–153.
5. N. Ryan, C. Heneghan, and P. De Chazal, (2004) , "Registration of digital retinal images using landmark correspondence by expectation maximization," vol. 22, pp. 883–898.
6. S. Fefilatyev, D. Goldgof, M. Shreve, and C. Lembke, (2012), "Detection and tracking of ships in open sea with rapidly moving buoy-mounted camera system," Ocean Engineering, vol. 54, pp. 1–12.
7. D. Bloisi, L. Iocchi, M. Fiorini, and G. Graziano, (2011), "Automatic maritime surveillance with visual target detection," Proc. International Defense and Homeland.
8. E. Lataire, (2004), "Taking into account the influence of the wave elevation along the hull of a sailing yacht in the resistance prediction," Delft University of Technology, 2004.
9. S. Geerts, G. Kerkhove, M. Vantorre, and G. Delefortrie, (2011) "Waterline registration using fluorescent lighting," in Advanced Model Measurement Technology for EU Maritime Industry, pp. 61–69.
10. A. Khare, M. Saxena, and S. Tiwari, (2011), "Edge Detection Method for Image Segmentation – A Survey of Soft Computing Approaches," no. 4, pp. 174–178.
11. J. P. Lewis, (1995), "Fast normalized cross-correlation," in Industrial Light & Magic.
12. R. Hartley and A. Zisserman, (2003), Multiple view geometry in computer vision, 2nd Ed. Cambridge University press.
13. P. Truijens, (1992), "Studie ter bepaling van het gemiddeld golfklimaat in de omgeving van Zeebrugge," Dienst voor Scheepsbouwkunde, Ghent University.
14. M. Tello, S. Silva Ribeiro, and C. Guedes Soares, (2011), "Seakeeping performance of fishing vessels in irregular waves," Ocean Engineering, vol. 38, no. 5–6, pp. 763–773.